



— BUREAU OF —
RECLAMATION

Investigating the Effect of Post Processing Procedures on Corrosion Resistance of Additively Manufactured 316L Stainless Steel

Science and Technology Program

Research and Development Office

Final Report No. ST-2020-20035

Technical Memorandum No. 8540-2020-20035



REPORT DOCUMENTATION PAGE				<i>Form Approved</i> <i>OMB No. 0704-0188</i>	
The public reporting burden for this collection of information is estimated to average 1 hour per response, including the time for reviewing instructions, searching existing data sources, gathering and maintaining the data needed, and completing and reviewing the collection of information. Send comments regarding this burden estimate or any other aspect of this collection of information, including suggestions for reducing the burden, to Department of Defense, Washington Headquarters Services, Directorate for Information Operations and Reports (0704-0188), 1215 Jefferson Davis Highway, Suite 1204, Arlington, VA 22202-4302. Respondents should be aware that notwithstanding any other provision of law, no person shall be subject to any penalty for failing to comply with a collection of information if it does not display a currently valid OMB control number. PLEASE DO NOT RETURN YOUR FORM TO THE ABOVE ADDRESS.					
1. REPORT DATE (DD-MM-YYYY) 09-30-2020		2. REPORT TYPE Research		3. DATES COVERED (From - To) FY20 – FY20	
4. TITLE AND SUBTITLE Investigating the Effect of Post Processing Procedures on Corrosion Resistance of Additively Manufactured 316L Stainless Steel				5a. CONTRACT NUMBER 20XR0680A1-RY15412020PE20035/X0035	
				5b. GRANT NUMBER	
				5c. PROGRAM ELEMENT NUMBER 1541 (S&T)	
6. AUTHOR(S) Stephanie Prochaska, M.S., Materials Engineer				5d. PROJECT NUMBER ST-2020-20035 8540-2020-45	
				5e. TASK NUMBER	
				5f. WORK UNIT NUMBER 86-68540	
7. PERFORMING ORGANIZATION NAME(S) AND ADDRESS(ES) Materials and Corrosion Laboratory Technical Service Center Bureau of Reclamation U.S. Department of the Interior Denver Federal Center PO Box 25007, Denver, CO 80225-000				8. PERFORMING ORGANIZATION REPORT NUMBER 8540-2020-45	
9. SPONSORING/MONITORING AGENCY NAME(S) AND ADDRESS(ES) Science and Technology Program Research and Development Office Bureau of Reclamation U.S. Department of the Interior Denver Federal Center PO Box 25007, Denver, CO 80225-0007				10. SPONSOR/MONITOR'S ACRONYM(S) Reclamation	
				11. SPONSOR/MONITOR'S REPORT NUMBER(S) ST-2020-20035	
12. DISTRIBUTION/AVAILABILITY STATEMENT Final Report may be downloaded from https://www.usbr.gov/research/projects/index.html					
13. SUPPLEMENTARY NOTES					
14. ABSTRACT The open circuit potential of cold-rolled and additively manufactured (AM) 316L stainless steel was measured. The AM parts underwent a variety of post-processing procedures including grinding and polishing, heat treatment, and a novel sensitization and etching process (used to remove support material). Microstructures and surface roughness of each specimen were evaluated, and specimens also underwent testing in an x-ray diffractometer. The as-printed specimens had the best corrosion resistance and the heat-treated specimens had the worst.					
15. SUBJECT TERMS Additive Manufacturing, corrosion, 316L stainless steel, optimization					
16. SECURITY CLASSIFICATION OF:			17. LIMITATION OF ABSTRACT	18. NUMBER OF PAGES 27	19a. NAME OF RESPONSIBLE PERSON Stephanie Prochaska
a. REPORT U	b. ABSTRACT U	THIS PAGE U			19b. TELEPHONE NUMBER (Include area code) 303-445-2323

Mission Statements

The Department of the Interior (DOI) conserves and manages the Nation's natural resources and cultural heritage for the benefit and enjoyment of the American people, provides scientific and other information about natural resources and natural hazards to address societal challenges and create opportunities for the American people, and honors the Nation's trust responsibilities or special commitments to American Indians, Alaska Natives, and affiliated island communities to help them prosper.

The mission of the Bureau of Reclamation is to manage, develop, and protect water and related resources in an environmentally and economically sound manner in the interest of the American public.

Disclaimer

Information in this report may not be used for advertising or promotional purposes. The data and findings should not be construed as an endorsement of any product or firm by the Bureau of Reclamation, Department of Interior, or Federal Government. The products evaluated in the report were evaluated for purposes specific to the Bureau of Reclamation mission. Reclamation gives no warranties or guarantees, expressed or implied, for the products evaluated in this report, including merchantability or fitness for a particular purpose.

Acknowledgements

The Science and Technology Program, Bureau of Reclamation, sponsored this research. The author would also like to thank Dr. Owen Hildreth, Dr. Meredith Heilig, and the Hildreth Research Group at the Colorado School of Mines for their guidance and support.

Investigating the Effect of Post Processing Procedures on Corrosion Resistance of Additively Manufactured 316L Stainless Steel

Final Report No. ST-2020-20035

Technical Memorandum No. 8540-2020-45

prepared by

Technical Service Center

Materials and Corrosion Laboratory Group

Stephanie Prochaska, Materials Engineer

Peer Review

Bureau of Reclamation
Research and Development Office
Science and Technology Program

Final Report No. ST-2020-20035
Technical Memorandum No. 8540-2020-45

Investigating the Effect of Post Processing Procedures on Corrosion
Resistance of Additively Manufactured 316L Stainless Steel

Prepared by: Stephanie Prochaska, M.S.
Materials Engineer, Materials and Corrosion Laboratory, 86-68540

Technical Approval by: Grace Weber, M.S.
Materials Engineer, Materials and Corrosion Laboratory, 86-68540

Checked by: Matthew Jermyn
Materials Engineer, Materials and Corrosion Laboratory, 86-68540

Peer Review by: Jessica Torrey, Ph.D., P.E.
Group Manager, Materials and Corrosion Laboratory, 86-68540

“This information is distributed solely for the purpose of pre-dissemination peer review under applicable information quality guidelines. It has not been formally disseminated by the Bureau of Reclamation. It does not represent and should not be construed to represent Reclamation’s determination or policy.”

Acronyms and Abbreviations

Ag/AgCl	Silver/silver chloride
AM	Additive manufacturing
AP	As-printed
BCC	Body-centered cubic
C	Carbon
CR	Cold-rolled
Cr	Chromium
ETC	Sensitized/etched
FCC	Face-centered cubic
Fe	Iron
HNO ₃	Nitric acid
HT	Heat-treated
KCl	Potassium Chloride
Mo	Molybdenum
Na ₄ Fe(CN) ₆ ·10H ₂ O	Sodium hexacyanoferrate (II) decahydrate
Ni	Nickel
OCP	Open circuit potential
PBF	Powder bed fusion
Reclamation	Bureau of Reclamation
SHE	Standard hydrogen electrode
SLM	Selective laser melting
XRD	X-ray diffraction

Measurements

°C	degrees Celsius
g	grams
mg	milligrams
mL	milliliters
mm	millimeters
V	Volts
V _{SHE}	Volts relative to a standard hydrogen electrode
wt.%	Weight percent

Contents

	Page
Mission Statements	ii
Disclaimer	ii
Acknowledgements	ii
Peer Review	iii
Acronyms and Abbreviations	iv
Measurements	iv
Executive Summary	1
1. Introduction	2
1.1 Project Background	3
2. Technical Approach and Methods	3
2.1 Specimen Preparation	3
2.1.1 Cold rolled	3
2.1.2 As-printed	4
2.1.3 Heat treated	4
2.1.4 Sensitized/etched	4
2.2 Specimen Analysis	5
2.2.1 Open circuit potential measurements	5
2.2.2 Metallographic analysis	6
2.2.3 X-Ray Diffraction	6
2.2.4 Profilometry	7
3. Results and Discussion	7
3.1 Open Circuit Potential Measurements	7
3.1.1 Cold rolled	8
3.1.2 As-printed	8
3.1.3 Heat treated	9
3.1.4 Sensitized/etched	10
3.2 Metallographic Analysis	10
3.2.1 Cold rolled	10
3.2.2 Additively manufactured	11
3.2.2.1 As-printed	12
3.2.2.2 Heat treated	13
3.2.2.3 Sensitized/etched	14
3.3 X-Ray Diffraction	14
3.4 Profilometry	15
4. Conclusions	16
References	18
Data Supporting the Final Report	19

Executive Summary

Additive manufacturing has been identified as a potential pathway for fabricating obsolete mechanical components on Reclamation's aging infrastructure. Although Reclamation could develop the capability to print the needed metallic parts, post-processing of the complex geometries could be costly, time consuming, may not yield required design tolerances, and could initiate deleterious effects, such as corrosion. This study investigated the durability of additively manufactured replacement parts in Reclamation's corrosive service environments.

To determine the effect of various post-processing techniques on corrosion response in additively manufactured 316L stainless steel, researchers evaluated the open circuit potential, microstructure, phases, and surface roughness of cold-rolled and additively manufactured disk specimens. The post-processing techniques evaluated were as-received (cold-rolled)/as-printed (additively manufactured, polished and unpolished), as-printed plus a heat treatment (polished and unpolished), and as-printed plus a surface sensitization and chemical etching (unpolished).

In general, open circuit potential (OCP) measurements showed that heat treating the specimens made them much more susceptible to corrosion while the as-printed specimens were the most noble. This result may be partially explained by the microstructural findings. The unhomogenized grain structure of the as-printed specimen did not provide any quick paths for electrons to reach the substrate and also had a higher resistance to corrosive attack; the smaller-grained, heat-treated and sensitized/etched specimens had a higher density of grain boundaries for easier electron transport, and thus had more negative potentials. Additionally, the smaller grains may have allowed for an increase in carbide precipitation and subsequent chromium depletion, resulting in lower potentials. The correlation between grain size/grain boundary density and OCP could be further explored in future work.

X-ray diffraction confirmed the presence of pure austenitic steel as well as the presence of corrosive-attack-inducing carbide precipitates. Peak quantification—not performed in the present study—could reveal additional insight into the corrosion response of each specimen type. In particular, the ability to quantify the amount of chromium or other corrosion inhibitor present in the specimen could help to further explain the OCP results. Energy dispersive x-ray spectroscopy must also be performed to correlate element concentration with the corrosion potential of each specimen.

Surface roughness also influences corrosion response. The sensitization/chemical etching process provided the most consistently smooth surface of all printed specimens evaluated without the need for manual smoothing via grinding, polishing, or other methods. Polished specimens had worse corrosion resistance than their unpolished counterparts, which was an unexpected result. Additional testing should be conducted to confirm this result and to determine exact corrosion mechanisms.

1. Introduction

The cost for post-processing of additively manufactured (AM) parts includes the labor and equipment to remove the structural supports that support a piece during the AM process, and can account for more than 45 percent of the total cost of printing [1]. One novel solution to simplify post-processing was developed by Dr. Owen Hildreth at the Colorado School of Mines [2]. In this method, the chemical stability of the top 100-200 microns of the part's surface is decreased and is carburized during thermal annealing by exposing the part to sodium hexacyanoferrate (II) decahydrate ($\text{Na}_4\text{Fe}(\text{CN})_6 \cdot 10\text{H}_2\text{O}$) under certain heating conditions. The surface is made sensitive to chemical and electrochemical dissolution when the protective chromium in chromium carbide precipitates is captured during the reaction. Then, only the carburized layer of the part is selectively corroded when the entire part is submerged in a solution of nitric acid (HNO_3) and potassium chloride (KCl) and subjected to an anodic bias. On parts intended for service, support structures can be designed to be less than 200 microns in width so that they can be dissolved away by utilizing this method.

While the support dissolution process is proven to be successful at removing support material from stainless steel parts, it is unknown whether the corrosion resistance of the parts is maintained. This paper evaluates powder bed fusion (PBF) additively manufactured 316L steel specimens after they have undergone the sensitization and dissolution process. The corrosion response in sodium chloride (NaCl) of 316L powder bed fusion parts was evaluated as a function of post-processing parameters to better understand the material-process-structure relationship. This work also evaluated the surface roughness of a part before and after support dissolution. The goal of this work was to optimize the feasibility of using AM to print metal parts while ensuring printed parts could be utilized in the Bureau of Reclamation's (Reclamation) corrosive service environments.

Evaluated PBF specimens were printed at 0 degrees (horizontal) to the build platform. The specimens were tested as-printed, polished, heat treated, and after the sensitization and etching process. Those results were compared to a specimen of conventionally manufactured, cold rolled 316L stainless steel.

While there has been little work done to evaluate the corrosion response of PBF-manufactured 316L stainless steel parts subject to various post-processing parameters and build orientation, effect of print parameters has been well studied in NaCl electrolytes. Zhang et al. showed that while laser scan speed did not affect corrosion resistance, compared to wrought, corrosion resistance improved as the porosity of parts printed via selective laser melting (SLM, a PBF derivative) decreased [3]. Those results corroborated a 2014 work showing corrosion resistance of SLM printed parts being worse than that of wrought 316L steel when the porosity was greater than one percent [4]. Another study found that increasing porosity lowered the repassivation potentials and had no significant effect on pitting potentials [5]. Heat treatment of SLM 316L parts has also been shown to affect corrosion resistance. Heat treatment homogenized the structure of the steel and dissolved inclusions—which can act as local sites for corrosion pitting—thus improving the corrosion resistance compared to wrought steel [6].

1.1 Project Background

Reclamation's aging infrastructure is facing maintenance problems that extend well beyond the ability to preserve features utilizing protective coatings or other conservation techniques. Certain metal parts are beginning to need replacement, with AM identified as one possible way to fabricate them. Although Reclamation could easily develop the capability to print the needed parts, post-processing of the complex geometries could be too costly and time consuming for AM to be a feasible solution. In addition, some parts, like impeller blades and hydraulic pathways within generator air coolers, require certain design tolerances to function properly, which presents further barriers to Reclamation in utilizing AM to produce replacement parts.

The novel process developed by Dr. Hildreth has already been proven to selectively dissolve support structures, remove trapped powder, and improve the mechanical performance of AM parts. However, further investigation into the corrosion properties of parts subjected to this and other post-processing techniques will provide insight into the durability of additively manufactured replacement parts in Reclamation's corrosive service environments.

2. Technical Approach and Methods

The experiment utilized 316L stainless steel disks, 15 millimeters (mm) in diameter and 4 mm thick. One replicate of each polished and unpolished specimen type was tested. Tested disks included conventionally manufactured cold rolled 316L steel, 316L steel printed via a PBF process (as-printed), heat treated as-printed 316L steel, and as-printed 316L steel subjected to the sensitizing and etching procedure. Table 1 shows each manufacturing and post-processing technique evaluated in this work.

Table 1: Manufacturing and post-processing techniques evaluated

Manufacturing Technique	Post-Processing Technique	Polished	Unpolished
Cold rolled	N/A (as-received)	X	X
AM (PBF)	N/A (as-printed)	X	X
AM (PBF)	Heat treated	X	X
AM (PBF)	Sensitization/chemical etching		X

2.1 Specimen Preparation

2.1.1 Cold rolled

The cold rolled 316L stainless steel specimens were obtained from McMaster Carr. One specimen was ground and polished to a one-micron finish (mirror finish) on a Struers LaboForce-100 automatic polisher with a diamond suspension. A second specimen was tested in the as-received

(unpolished) condition. A VEVOR PS-30A Digital Ultrasonic Cleaner was used to ultrasonically clean the specimens for five minutes in isopropyl alcohol.

2.1.2 As-printed

The as-printed stainless steel specimens were manufactured by Elementum 3D in Erie, Colorado, via a PBF process. One specimen was ground and polished to a one-micron finish using diamond suspension. A second specimen was tested in the as-received (as-printed) condition. Specimens were ultrasonically cleaned for five minutes in isopropyl alcohol.

2.1.3 Heat treated

Typically, AM parts would not be used in their as-printed state. Most AM metal parts undergo a heat treatment scheme to relieve stress built up during the printing process and homogenize the microstructure, imparting better mechanical properties and overall improving part performance.

As-printed PBF specimens from the same batch as specimens described in 2.1.2 were heat treated in a Thermo Scientific Lindberg Blue M tube furnace. Starting at room temperature, the ramp rate was 10 degrees Celsius (°C) per minute to 950 °C. The temperature was held at 950 °C for two hours and then the specimens were removed from the furnace and quenched in air at room temperature to preserve the microstructure [7]. One specimen was ground and polished to one micron. A second heat-treated specimen that did not undergo grinding or polishing was also tested. Specimens were ultrasonically cleaned for five minutes in isopropyl alcohol.

2.1.4 Sensitized/etched

The sensitized/etched 316L stainless steel specimens used for this portion of the study were from the same batch as the printed specimens described in 2.1.2. The sensitizing and etching parameters described below were experimentally determined through previous studies.

To sensitize the printed 316L stainless steel specimens, a saturated solution of $\text{Na}_4\text{Fe}(\text{CN})_6 \cdot 10\text{H}_2\text{O}$ ($\geq 99\%$; Alfa Aesar) and deionized water was prepared. In addition, a paste of 4.2 parts by mass $\text{Na}_4\text{Fe}(\text{CN})_6 \cdot 10\text{H}_2\text{O}$ and one-part deionized water was also prepared. The specimens were submerged in the saturated solution for 20 minutes and then completely coated with the 4.2:1 paste. The coated specimens were wrapped tightly with a high temperature tool wrap (MSC Industrial Supply, 309 stainless steel tool wrap). A small hole, approximately 0.1-mm in diameter, was punched into the corner of the tool wrap to allow for the release of cyanide and water vapor that is formed during the decomposition of the paste. The tool wrap-and-specimen package was placed in a Lindberg Model C10 silicon carbide box furnace at room temperature. The furnace was heated with a ramp rate of 5 °C per minute to 800 °C. The package remained at that temperature for six hours; then, the furnace was turned off and allowed to cool to room temperature.

To etch the sensitized specimens, they were first removed from the tool wrap package and ultrasonicated in deionized water for five minutes. The specimens were then secured in a specially made sample holder. An electrolyte solution of 0.48 molar concentration HNO_3 and 0.1 molar concentration of KCl (28.52 milliliters (mL) HNO_3 and 6.7 grams (g) KCl in 900 mL deionized water) was prepared. The electrolyte was poured into a corrosion cell and the specimen in the sample holder was placed into the cell. A silver/silver chloride (Ag/AgCl) reference electrode was ionically connected to the electrolyte through a KCl salt bridge. The counter electrode was a 6-mm diameter graphite rod.

A Princeton Applied Research Parstat MC potentiostat was utilized to perform chronoamperometry with a potential of -0.01 Volts (V) for 60 seconds to clean the specimen's surface. The open circuit potential (OCP) was then measured for 200 seconds and cyclic voltammetry curves were generated. Finally, the etching process was initiated through chronoamperometry at a potential of 0.2 V for a duration of 50 hours. Once the etching was complete, the specimens were ultrasonically cleaned in deionized water for five minutes. The etched specimens were not ground or polished.

Figure 1 shows each specimen type after preparation (polished versions not shown). Note the slight change in color of the heat-treated and sensitized/etched specimens which is due to diffusion of carbon to the specimens' surfaces.



Figure 1: 316L stainless steel specimens. From left: cold rolled steel, as-printed PBF printed steel, heat treated PBF printed steel, and PBF printed steel after sensitization and etching.

2.2 Specimen Analysis

2.2.1 Open circuit potential measurements

To prepare specimens for OCP measurements, conductive copper wire leads were attached to the specimens' surfaces with silver epoxy. Then, the specimens with attached leads were cold mounted in epoxy. OCP was measured with a potentiostat for a duration of 50 hours. The electrolyte solution was 3.5 wt. % NaCl in deionized water. An Ag/AgCl reference electrode was ionically connected to the electrolyte through a KCl salt bridge. The counter electrode was a 6-mm diameter graphite rod. Figure 2 shows the test cell set up for the OCP measurements, which was functionally equivalent to the set up utilized during the etching process.

Measured potentials were offset by +0.197 V so they could be reported relative to the standard hydrogen electrode (SHE).

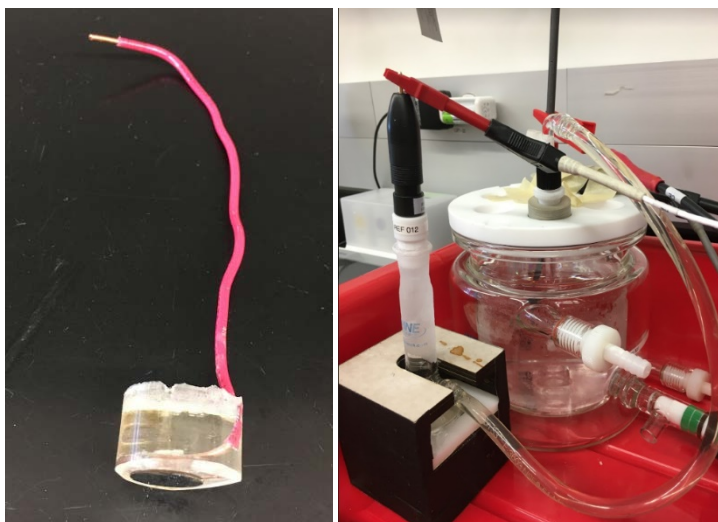


Figure 2: Specimen connected to a copper wire lead and mounted in epoxy (left) and electrochemical measurement set up (right).

2.2.2 Metallographic analysis

Specimens for metallographic analysis were cold mounted in epoxy resin. Specimens were cut in half and oriented so the cross section and surface face of the disk could both be evaluated (Figure 3). Mounted specimens were ground and polished to a one-micron surface finish. Polished specimens were stain etched in glyceric acid (a 3:2:1 ratio of hydrochloric acid, glycerin, and HNO_3) for 1 minute and 20 seconds to reveal grain structure, carbides, and phases.



Figure 3: Metallography specimen (as-printed) mounted in epoxy and polished to one micron.

2.2.3 X-Ray Diffraction

X-ray diffraction (XRD) was performed on a Bruker AXS D2 Phaser diffractometer from 27 to 130 two theta.

2.2.4 Profilometry

The surface roughness of the specimens was measured using a Bruker DektakXT profilometer. The scan resolution was 0.056 microns and stylus force was 3 milligrams (mg). Six 1000-micron long measurements were taken per specimen and the results were averaged.

3. Results and Discussion

3.1 Open Circuit Potential Measurements

Figure 4 shows the resulting “galvanic series” for all specimens tested. Specimens with more negative OCP measurements after 50 hours are more anodic and more susceptible to corrosion (relative to other specimens) whereas more positive OCP measurements indicate the specimens are more noble and are less susceptible to corrosion. In addition, in humid or salty environments, galvanic corrosion can occur between two dissimilar metals when their difference in potential is approximately 0.15 V or more [8]. Overall, heat treating the specimens made them much more susceptible to corrosion while the as-printed specimens were the most noble. This finding is surprising because unhomogenized microstructures (as in the as-printed specimens) contain regions of depleted chromium. Chromium is one of the main corrosion inhibitors in stainless steel. However, the heat treated specimens were at a high enough temperature to induce chromium carbide precipitation to the grain boundaries which can also result in regions of chromium depletion and, subsequently, increase susceptibility to corrosion attack.

Increasing susceptibility to corrosive attack ↑	V_{SHE}	Specimen
	-0.025	Heat Treated (polished)
	0.000	Sensitized/Etched (from 0-40 hours)
	0.025	Heat Treated (unpolished)
	0.125	Cold Rolled (polished)
	0.150	As-printed (polished)/ Sensitized/Etched (40+ hours)
	0.200	Cold Rolled (unpolished)
	0.250	As-printed (unpolished)

Figure 4: Resulting galvanic series for all specimens evaluated in 3.5 wt.% NaCl for 50 hours. Specimens are listed from most susceptible to corrosive attack to least susceptible.

The polished version of each specimen type had more negative potentials than their unpolished counterparts. This result was unexpected since pits on rougher surfaces can render them more anodic by acting as corrosion concentration cells. However, one possible explanation is the disruption of the steel’s passivation layer due to polishing. While specimens did not undergo electrochemical evaluation until 24-48 hours after polishing, the passivation layer may not have had enough time to sufficiently regrow. Additional work must be performed to identify the exact mechanisms that are causing these unexpected phenomena to occur, and to evaluate the effect of

passivation layer thickness on OCP. Further discussion of the potential versus time curves for individual specimen types is included below.

3.1.1 Cold rolled

Figure 5 shows the potential versus time curve for the polished and unpolished (as-received) cold rolled specimens. After 50 hours, the potential of the unpolished specimen was $+0.2 V_{SHE}$ while the potential of the polished specimen was approximately $+0.125 V_{SHE}$. These measured potentials are slightly more positive than results noted in literature (typically 0 to $+0.1 V_{SHE}$) [9]. Both curves stabilize after approximately 15 hours of testing and remain relatively stable for the remainder of the evaluation period.

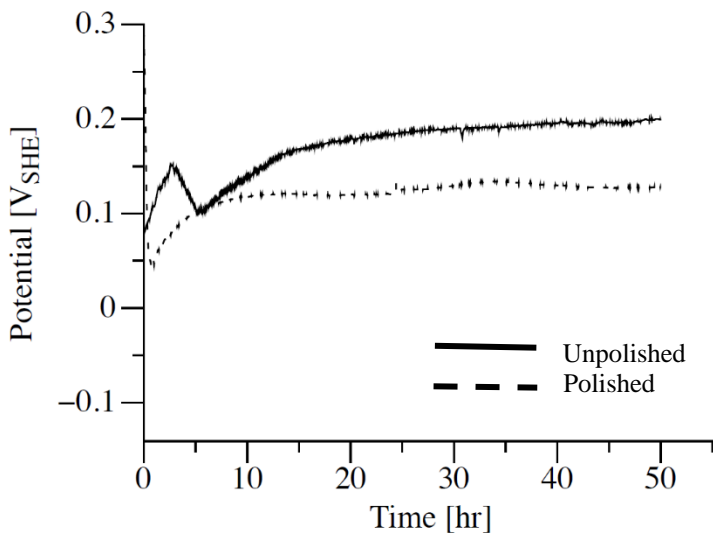


Figure 5: OCP curve for polished and unpolished cold rolled specimens.

3.1.2 As-printed

Figure 6 shows the potential versus time curve for the polished and unpolished as-printed specimens. The potential of the unpolished specimen was $+0.25 V_{SHE}$ and the potential of the polished specimen was $+0.15 V_{SHE}$ after 50 hours. Both polished and unpolished curves were relatively stable throughout the evaluation period—extremely negative potentials in the unpolished curve (i.e. at hours 12, 45, and 48) were likely due to external factors unrelated to the specimen's OCP, and overall did not affect the result after 50 hours. More moderate fluctuations in the unpolished curve could be due to the formation and dissolution of corrosion concentration cells that formed in surface divots.

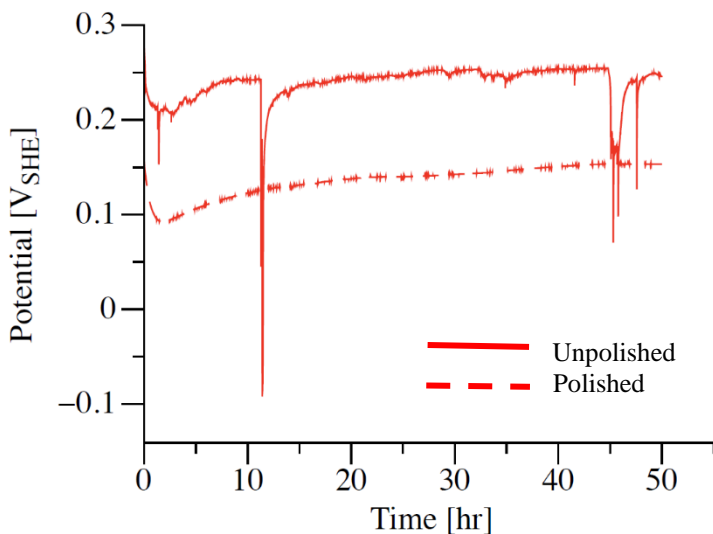


Figure 6: OCP curves for as-printed polished and unpolished specimens.

3.1.3 Heat treated

Figure 7 shows the potential versus time curves for the polished and unpolished heat-treated specimens. The potential of the unpolished specimen was approximately $+0.025 V_{SHE}$ and the potential of the polished specimen was approximately $-0.025 V_{SHE}$ after 50 hours of testing. Both curves stabilized after approximately 15-20 hours of evaluation.

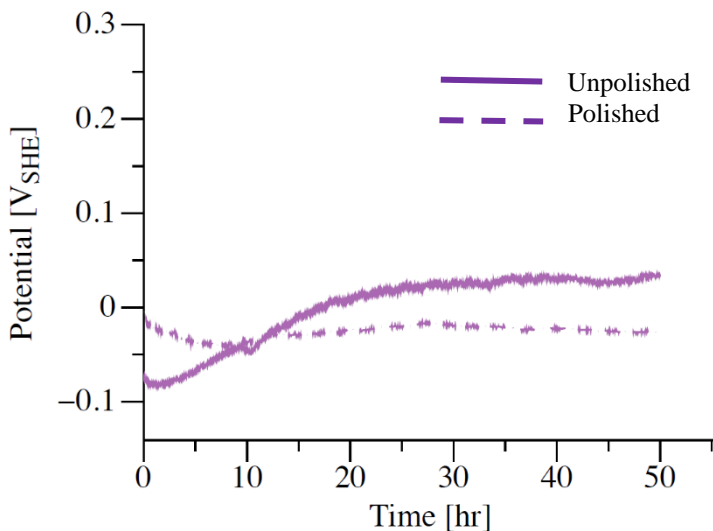


Figure 7: OCP curve for polished and unpolished heat-treated disks.

3.1.4 Sensitized/etched

Figure 8 shows the potential versus time curve for the unpolished sensitized/etched specimen. From approximately 5 to 40 hours, the potential oscillated around 0 V_{SHE}. This oscillation is likely due to the formation and subsequent destruction of a passivation layer on the specimen's surface. After 40 hours, the potential quickly became more positive to over +0.125 V_{SHE} and continued to become more positive throughout the last 10 hours of the evaluation. OCP evaluations exceeding 50 hours should be conducted to determine a stabilized potential (if any) at times longer than 50 hours. A more detailed electrochemical analysis must also be performed to determine the cause of the sharp change in potential observed herein. One theory is that a more permanent or thicker passivation layer formed on the surface after hour 40 and was not subsequently destroyed, thus rendering the potential more positive and improving resistance to corrosive attack.

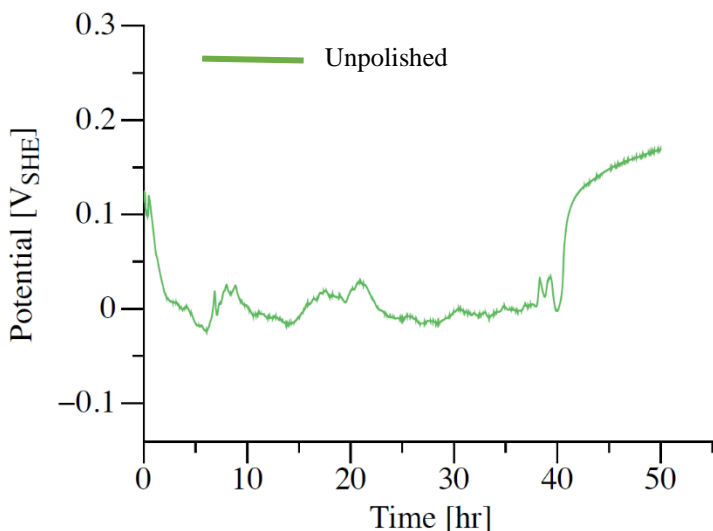


Figure 8: OCP curve for the sensitized/etched specimen.

3.2 Metallographic Analysis

3.2.1 Cold rolled

Figure 9 shows the typical microstructure of cold-rolled 316L stainless steel at a magnification of 12.6X and 63X (inset). Grains are typically no larger than 50 microns in diameter and are relatively uniform in size and shape. Due to the nature of the cold-rolling process, most grains appear to be elongated in one direction, whereas others retain their coaxial perimeters. Smaller grains are typically more favorable for the mechanical properties of steels. As grain size decreases, hardness, tensile strength, yield strength, and impact strength increase [10]. However, it has also been shown that as grain size decreases corrosion susceptibility increases. This phenomenon is due to the increased density of grain boundaries which act as “express lanes” to and from the surface for electrons and other diffusing species [11].

The micrograph also shows the presence of annealing twins. As recrystallization defects, annealing twins can be formed through many mechanisms. They can be particularly dense in FCC materials due to the various atomic stacking faults that can occur between the {111} planes. Annealing twins

lower the grain boundary energy and, if present in large enough quantities, can improve the mechanical properties of the steel.

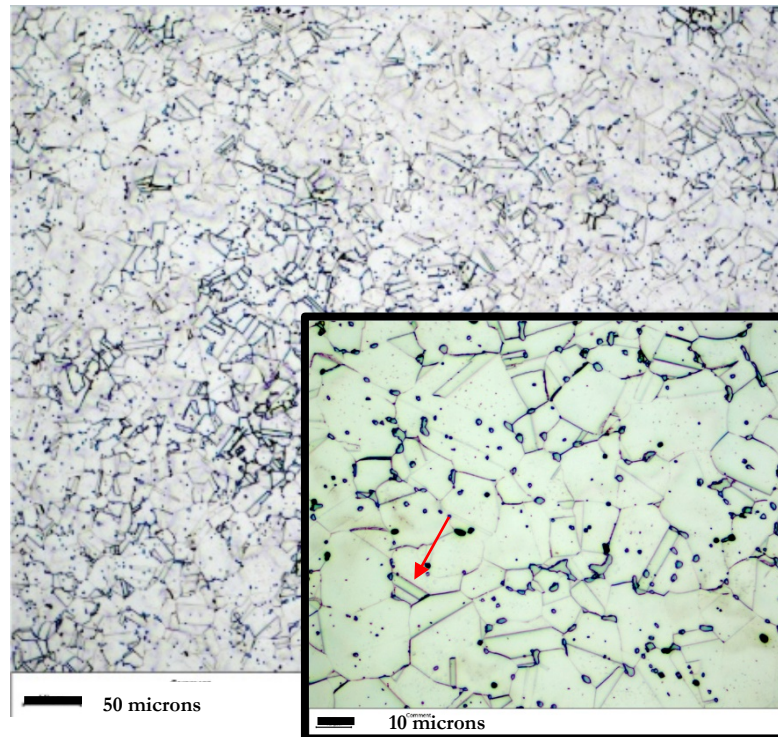


Figure 9: Observed near-surface microstructure of cold-rolled 316L stainless steel at a magnification of 12.6X and 63X (inset). Arrow indicates location of one instance of annealing twins.

Specific allotropes (phases) of iron present can be confirmed via XRD analysis. The body-centered cubic (BCC) α -Fe and face-centered cubic (FCC) γ -Fe are typical for steels, although γ -Fe (also known as austenite) is expected to be the dominant phase for 316L (austenitic) stainless steels [12]. Due to the larger size of FCC interstitial sites, austenite is characterized by its ability to absorb a significant amount of carbon. The carbon can then precipitate out of the interstitials and appear in the micrographs as small precipitate carbides (solid dark regions within grains and grain boundaries). When dispersed evenly throughout the matrix, carbides can improve corrosion resistance; however, corrosion resistance is impacted under certain annealing conditions which segregate carbides to grain boundaries. The tiny bound regions that are not completely solid in color are δ -Fe or sigma phase (a derivative of δ -Fe, hard and brittle intermetallic phase of chromium and iron). Presence of sigma phase is typically unfavorable as it can decrease a steel's corrosion resistance, as well as its ductility and toughness.

3.2.2 Additively manufactured

Figure 10 shows the near surface (top) and cross-section (bottom) micrographs for as-printed, heat treated, and sensitized/etched specimens at a magnification of 12.6X. Each specimen was evaluated at five different magnifications, and the micrographs included in the figure were selected to be the most representative of each surface. Some general observations can be made. The melt pools formed during the sintering of powder are clearly seen in the as-printed micrographs; these features

appear as parallel beads in the near surface micrograph and scallop-like in the cross-section view. Applying a heat treatment to the specimens completely dissolved the melt pools, homogenized the microstructure, and revealed the resulting grains.

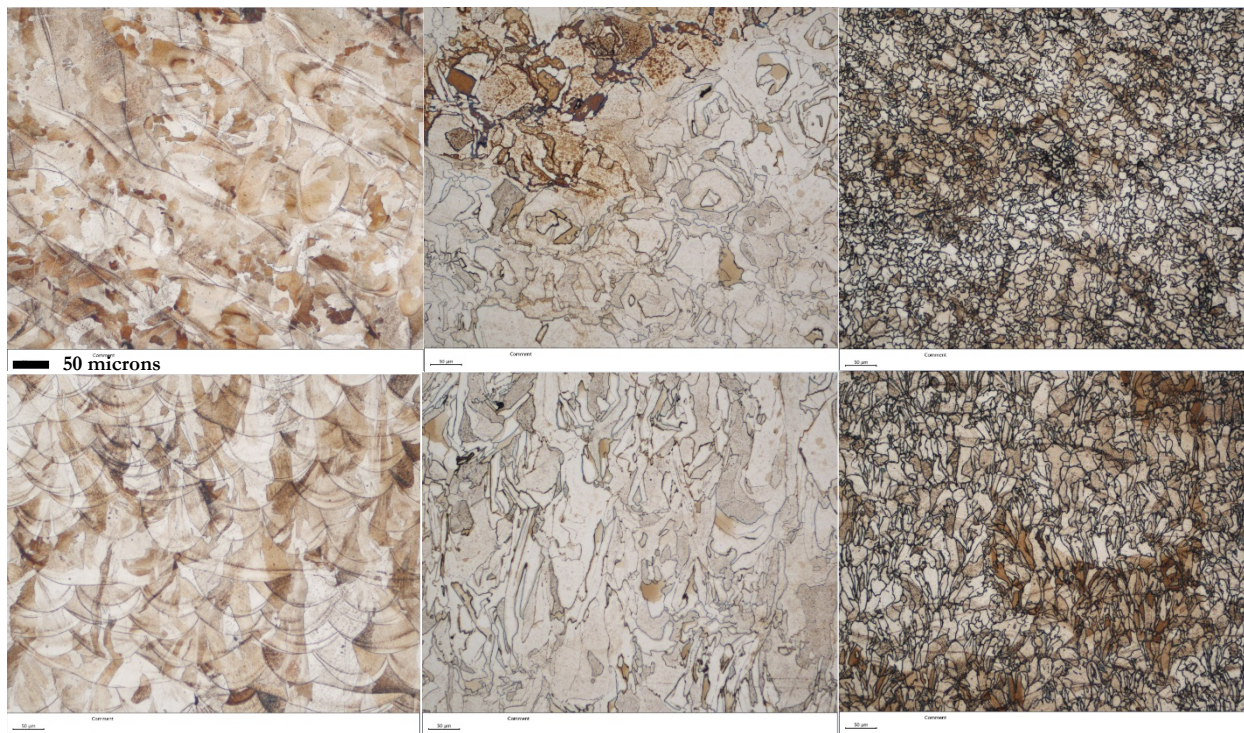


Figure 10: Near surface (top) and cross-sectional (bottom) microstructures of as-printed (left), heat treated (center), and sensitized/etched (right) specimens.

While grain growth increases with increasing temperature, the nucleation rate of new grains peaks at intermediate temperatures and then decreases [11]. This may partially explain why the grains of the heat-treated specimen (annealed at 950 °C) are larger and coarser than the grains of the sensitized/etched specimen (annealed at 800 °C). The sensitized/etched specimen's longer annealing time could have allowed the microstructure more time to achieve grain uniformity. In addition, the presence of precipitates can hinder grain growth, although their presence in each specimen type evaluated was not quantified as part of this study. Cooling rate differences may have also contributed to the differing microstructures.

Aside from the annealing component of the process, the surface sensitization and chemical etching likely did not greatly affect the sensitized/etched specimen's sub-surface microstructure. Future work could include microstructural analysis conducted directly on sensitized/etched specimen surface. Additional interesting microstructural features for each specimen type are noted below.

3.2.2.1 As-printed

A closer look at the as-printed cross section microstructure at a magnification of 63X (Figure 11) reveals the formation of regions with lamellar-like/dendritic structures. These structures are columnar grains formed due to directional solidification and are commonly seen in as-printed AM microstructures. Columnar grains typically grow in clusters with orientations that follow the thermal

gradient of the print process and are relatively fine due to higher cooling rates. This type of grain structure can give a material anisotropic mechanical properties—high plasticity but low strength [13].

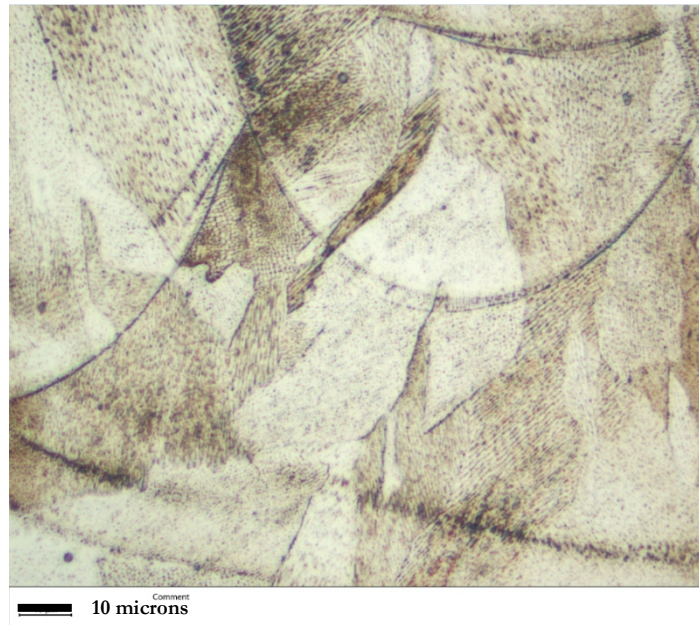


Figure 11: Microstructure of the as-printed specimen at a magnification of 63X.

3.2.2.2 Heat treated

Heat treating the disks at a temperature above the eutectic temperature resulted in a microstructure that is predominantly γ -Fe. A small amount of sigma phase and/or carbide precipitates are also seen along grain boundaries in Figure 12.



Figure 12: Microstructure of the heat-treated specimen at a magnification of 63X.

3.2.2.3 Sensitized/etched

The phases present in the sensitized/etched microstructure are also likely to be predominately γ -Fe. The microstructure also shows the presence of carbide precipitates and possible sigma phase. In addition to the much smaller grain sizes, annealing twins are visible in Figure 13.

Previous studies have found that the small grained microstructure of the sensitized/etched specimens provided enhanced mechanical properties to cold rolled 316L stainless steel [2].

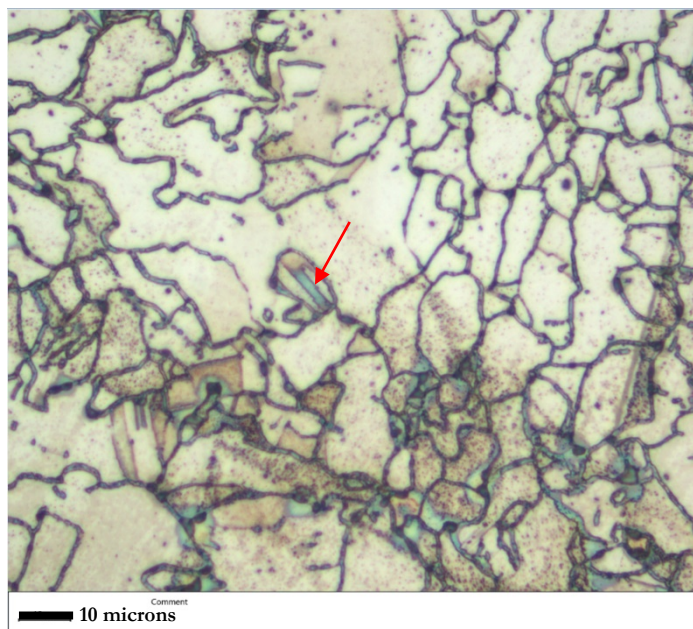


Figure 13: Microstructure of the sensitized/etched specimen at a magnification of 63X. Arrow indicates location of one instance of annealing twins.

OCP measurements may be partially explained by the microstructural findings. The unhomogenized grain structure of the as-printed specimen did not provide any quick paths for electrons to reach the substrate and also had a higher resistance to corrosive attack; the smaller-grained heat-treated and sensitized/etched specimens had a higher density of grain boundaries for easier electron transport and thus had more negative potentials. The correlation between grain size/grain boundary density and OCP could be further explored in future work.

3.3 X-Ray Diffraction

Diffraction peaks for all specimens are shown in Figure 14. As expected, all specimens showed similar peaks except for the etched/sensitized specimen which had a few additional peaks. The XRD results showed the characteristic peaks associated with austenitic steel. The etched/sensitized specimen also showed the presence of carbides which were visual on the surface and noted in the micrographs. Peak quantification—not performed in the present study—could reveal additional insight into the corrosion response of each specimen type. In particular, the ability to quantify the

amount of chromium or other corrosion inhibitor present in the specimen could help to further explain some OCP results.

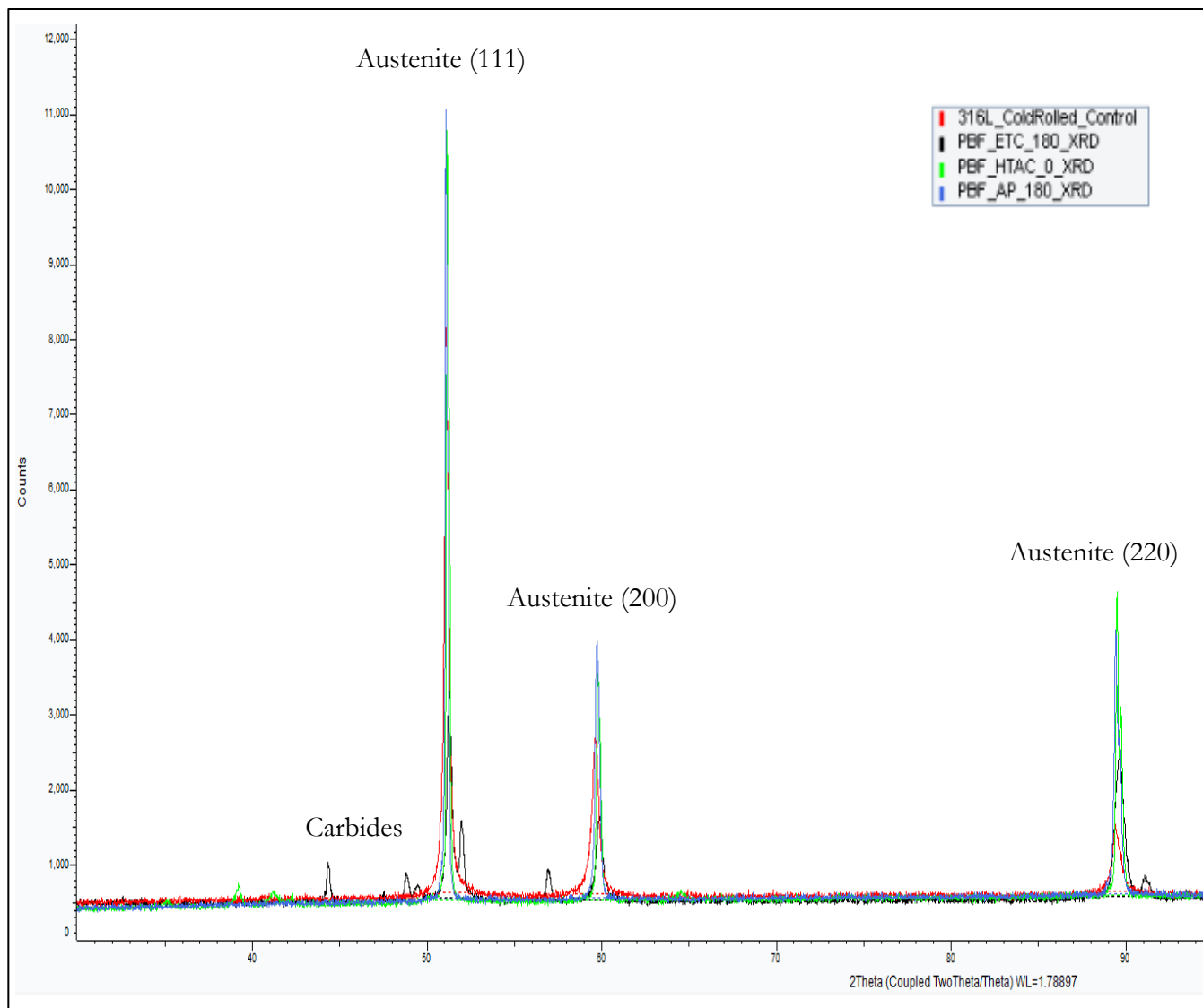


Figure 14: Observed diffraction peaks for all specimens. For enhanced readability, plot has been truncated to show only the peaks from 30 to 95 2-theta. Peaks above 95 2-theta were typical for 316L stainless steel.

3.4 Profilometry

Figure 15 shows the results of the profilometry measurements for the cold rolled and printed disks subject to the various post-processing procedures. All polished specimens had, on average, a roughness value of 0.01 microns and were not included in the plot.

The cold rolled (CR) specimen had an average roughness value of 2.66 microns and a standard deviation of 0.65 microns. The average roughness value for the as-printed (AP) specimen was nearly double that of the cold rolled at 4.9 microns but had a similar standard deviation of 0.63 microns. The heat treated (HT) specimen had the highest average roughness value at 6.7 microns as well as the largest standard deviation (1.2 microns), this is potentially due to the precipitation of carbides onto the surface. The etched/sensitized (ETC) specimen had the lowest average roughness value of all printed specimens and lowest standard deviation of all specimens tested, 3.74 and 0.22 microns, respectively. Similarly to the heat-treated specimens, carbides precipitated on the surface during the specimen sensitization, but the protrusions were then preferentially removed during the etching process, leaving behind a smoother surface.

The sensitization/etching process provided the most consistently smooth surface of all printed specimens evaluated without the need for manual smoothing via grinding, polishing, or other methods.

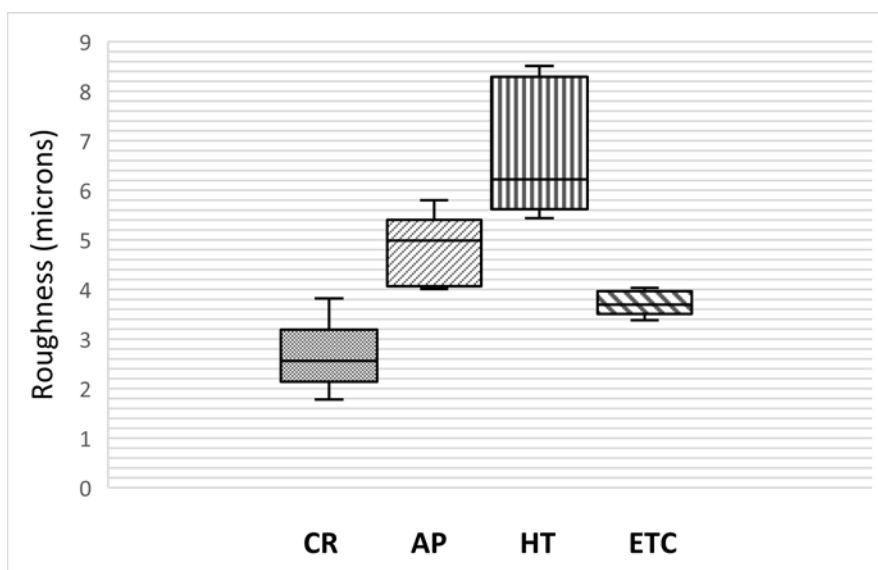


Figure 15: Box and whisker plots showing profilometry results for all unpolished specimens.

4. Conclusions

- As part of a larger effort to explore the potential for implementing AM at Reclamation, this work has shown that various post-processing techniques of AM 316L stainless steel result in different microstructures, surface conditions, and corrosion responses from conventionally manufactured steel. This proof of concept exemplifies how Reclamation cannot simply replace a conventionally manufactured part with a part manufactured via AM without considering the broader implications of both the mechanical and environmental interactions of the AM material. While some generalizations can be made, additional work must be completed before Reclamation can implement these results.
- The as-printed specimens were the least susceptible to corrosive attack, suggesting 316L stainless steel parts should be utilized in their as-printed condition if corrosion resistance is

the main concern. However, this is never recommended because the microstructure of as-printed parts is typically un-developed or under-developed and residual stresses must be relieved via annealing.

- Through 40 hours of OCP evaluation, the sensitized/etched specimen held stable at potentials similar to the polished as-printed specimen, but additional work must be done to explain the positive potential shift between 40 and 50 hours and to determine the OCP behavior past 50 hours.
- Polished surfaces were more susceptible to corrosive attack compared to their unpolished counterparts. Additional replicates must be tested to confirm this result and further work needs to be done to identify the exact corrosion mechanisms.
- XRD confirmed the presence of corrosive-attack inducing carbide precipitates as well as corrosion inhibiting chromium, but peak quantification as well as energy dispersive x-ray spectroscopy must be performed to determine the extent of the effect that these species have on the corrosion potential of each specimen.
- The sensitization/etching process provided the most consistently smooth surface of all printed specimens evaluated without the need for manual smoothing via grinding, polishing, or other methods.

References

- [1] B. Post, R. Lind, P. Lloyd, V. Kunc, J. Linhal and L. Love, "The Economics of Big Area Additive Manufacturing," in *Solid Freeform Fabrication Symposium--An Additive Manufacturing Conference*, Austin, 2016.
- [2] C. Lefky, B. Zucker, W. Wright, A. Nassar, T. Simpson and O. Hildreth, "Dissolvable Supports in Powder Bed Fusion-Printed Stainless Steel," *3D Printing and Additive Manufacturing*, vol. 4, no. 1, pp. 2-11, 2017.
- [3] Y. Zhang, F. Liu, J. Chen and Y. Yuan, "Effects of surface quality on corrosion resistance of 316L stainless steel parts manufactured via SLM," *Journal of Laser Applications*, vol. 29, p. 022306, 2017.
- [4] Y. Sun, A. Moroz and K. Alrbaey, "Sliding Wear Characteristings and Corrosion Behaviour of Selective Laser Melted 316L Stainless Steel," *Journal of Materials Engineering and Performance*, vol. 23, no. 2, pp. 518-526, 2014.
- [5] G. Sander, S. Thomas, V. Cruz, M. Jurg, N. Birbilis, X. Gao, M. Brameld and a. C. R. Hutchinson, "On The Corrosion and Metastable Pitting Characteristics of 316L Stainless Steel Produced by Selective Laser Melting," *Journal of the Electrochemical Society*, vol. 164, no. 6, pp. C250-C257, 2017.
- [6] Q. Chao, V. Cruz, S. Thomas, N. Birbilis, P. Collins, A. Taylor, P. Hodgson and D. Fabijanac, "On the enhanced corrosion resistance of a selective laser melted austenitic stainless steel," *Scripta Materialia*, vol. 141, pp. 94-98, 2017.
- [7] M. M. Sistiaga, S. Nardone, C. Hautfenne and J. V. Humbeeck, "Effect of Heat Treatment of 316L Stainless Steel Produced by Selective Laser Melting (SLM)," in *International Solid Freeform Fabrication Symposium*, Austin, 2016.
- [8] A. Pirolini, "Galvanic Corrosion of Steel and other Metals," AZO Materials, 11 March 2015. [Online]. Available: <https://www.azom.com/article.aspx?ArticleID=11833>. [Accessed 11 September 2020].
- [9] C. Compere and N. Lebozec, "Behaviour of stainless steel in natural seawater," in *The First Stainless Steel Congress in Thailand*, Bangkok, 1997.
- [10] M. Soleimani, H. Mirzadeh and C. Dehghanian, "Effect of grain size on the corrosion resistance of low carbon steel," *Materials Research Express*, vol. 7, no. 016522, 2020.
- [11] R. W. Balluffi, S. M. Allen and W. C. Carter, *Nucleation*, Hoboken: John Wiley & Sons, Inc., 2005, pp. 459-484.
- [12] Total Materia, "Microstructures in Austenitic Stainless Steels," Total Materia, March 2010. [Online]. Available: <https://www.totalmateria.com/page.aspx?ID=CheckArticle&site=kts&LN=EN&NM=268>. [Accessed 2 September 2020].
- [13] W. Kun, W. Dan and H. Fusheng, "Effect of crystalline grain structures on the mechanical properties of twinning-induced plasticity steel," *Acta Mechanica Sinica*, vol. 32, no. 1, pp. 181-187, 2016.

Data Supporting the Final Report

Data from this project is stored within folders at the following file path:

T:\Jobs\DO_NonFeature\Science and Technology\2020-PRG-Corrosion Reliability of Additively Manufactured 316L Stainless Steel

- Point of Contact: Stephanie Prochaska, sprochaska@usbr.gov, 303-445-2323
- Data saved for this project includes x-ray diffraction peaks, raw profilometry measurements, micrographs of the specimens in multiple magnifications, and raw open circuit potential data. Data file types are .CSV, .PNG, .TIF, and .PAR.
- Data was predominantly collected in the Hildreth Research Laboratory at the Colorado School of Mines between January and September 2020.
- Keywords: x-ray diffraction, profilometry, open circuit potential, additive manufacturing, microstructure, micrograph
- Approximate total size of all files: 523 MB

